Proceedings of the ASME 2014 33rd International Conference on Ocean, Offshore and Arctic Engineering
OMAE2014
June 8-13, 2014, San Francisco, California, USA

OMAE2014-23075

EFFECTS OF ATTRITION DUE TO WATER IN CYCLICALLY LOADED GROUTED JOINTS

Peter Schaumann **Alexander Raba** **Anne Bechtel**

ForWind – Center for Wind Energy Research
Institute for Steel Construction, Leibniz University Hannover
Germany

ABSTRACT

According to political goals, electricity from offshore wind farms in Germany will amount to 15 GW by 2030. Most of the wind farms will be located far offshore in water depths larger than 30 m. For such water depths, lattice substructures like jackets or tripods are the preferred solution. The substructures are founded on piles and connected to these by submerged grouted joints. In lattice substructures grouted joints are predominantly loaded by cyclic axial loads. Even though, this connection is well known from the offshore oil and gas industry, comparatively few results on effects of attrition due to water for grouted joints are available.

At the Institute for Steel Construction of the Leibniz University Hannover, Germany, within the joint research project 'GROWup' investigations focus on the fatigue performance of grouted joints under predominant axial loading. As part of this research project, cyclic loading tests on small scale grouted joints with shear keys were conducted. The specimens were filled with industrial grout products and tested in a water basin to evaluate the influence of water to the fatigue performance of the connection at small scale. These test results show that the water effect leads to a significant reduction of the fatigue performance of the connection compared to results from tests in dry conditions. Moreover, the impact of water is proportional to the applied test frequency. The results of the structural tests differ from results of pure material specimen tests, on which current code provisions are based.

This paper presents results from the small scale tests on grouted joints with shear keys in dry and submerged conditions. Effects of attrition due to water are shown and their effect is quantified. The results are compared to other published findings. In conclusion the presented investigations underline the importance of the water effect to the fatigue performance of small scale grouted joints. In conclusion, this paper will stimulate discussions on the demand for research on large- and real-scale grouted joints.

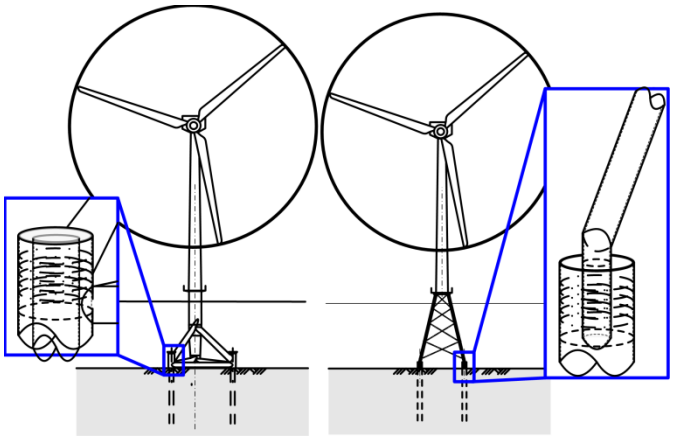

Figure 1: Grouted joints in tripod (left) and jacket (right) substructures for OWTs [1]

1 INTRODUCTION

With commencement of the German electricity feed-in law (Stromeinspeisegesetz, SEG) in 1991 the electrical grid was opened for smaller independent power producers and the expansion of renewable energies in Germany was inspired. In 2009 alpha ventus (60 MW) the first offshore wind farm in Germany's exclusive economic zone was commissioned, followed by EnBW Baltic 1 in 2011 (~50 MW) and BARD Offshore 1 in 2013 (400 MW) [2]. About 30 more wind farm projects, with an overall capacity of about 8 GW, are already approved and about 60 more are in the approval procedure, mainly located in Germany's Exclusive Economic Zone (EEZ) in the North Sea.

The lessons learned while realizing the first wind farms show possibilities for further research and development concerning all stages from planning, over realization to grid integration. As a result the German government, newly elected in September 2013, decided to reduce the prior expansion

targets for offshore wind energy from 25 GW installed capacity in the year 2030 to more realistically 15 GW [3]. Nevertheless, a capacity of about 1 GW per year will have to be installed to reach the new target. The current standard offshore wind turbine (OWT) has a capacity of 5 MW, so this means about 200 OWTs will have to be erected per year.

The building areas for offshore wind farms in the EEZ are under administration of the German Maritime and Hydrographic Agency (BSH). In their Maritime Spatial Plan for the North Sea [4] the building areas are mainly located in water depths of 30 m and deeper. For such water depths, lattice substructures like jackets or tripods (cf. Figure 1) are the preferred solution up to now.

The substructures are founded on steel piles which are driven into the seabed. To connect the piles and the substructure a composite connection called grouted joint, explained in section 2, is applied. Due to the configuration of the substructure the acting loads from wind, waves, operation and dead loads are split into couples of axial forces acting on the grouted joint.

Even though, prevailingly axial loaded grouted joints are utilized in the oil and gas industry for many years now, three main aspects are different for OWTs. Firstly, the geometric dimensions of the joints are larger and stiffness relations change. Secondly, the filling material grout has changed from low strength cement slurries to high performance grouts with aggregates. And thirdly, alternating loads from wind and waves become the dominating action and therefore, deeper understanding of the fatigue behaviour of the grouted connection is needed.

Moreover, the grouted joints are located just above the mudline and therefore, are always submerged. Earlier research focused on the influence of water to the fatigue behaviour of plain concrete structures and materials (cf. [5–8]). All of these works found out that water reduces the fatigue life. To what extend these results can be transferred to grouted joints as a structural detail has not been investigated yet.

The research project ‘GROWup – grouted joints for Offshore Wind Energy Converters under reversed axial loadings and up scaled thicknesses’ (funding sign: 0325290) funded by the German Federal Ministry for the Environment, Nature Conservation and Nuclear Safety (BMU) is the third research project in a row at the Leibniz University in Hannover, Germany focusing on grouted joints for OWTs. The Institute for Steel Construction investigates the structural behaviour and in particular the fatigue performance in submerged conditions of grouted connections. Hereinafter, the results for small scale specimens are presented.

2 GROUTED JOINTS

The typical grouted joint consists of three main parts, as shown in Figure 2. A steel tube with a smaller diameter (pile) is inserted into a steel tube with a bigger diameter (sleeve) and the resulting annulus is filled with grout. The opposing tube surfaces are equipped with shear keys made of weld beads.

Acting loads are transferred from tube to grout via interlocking between the shear keys and the grout. Within the grout the loads are passed on via shear. Between opposing shear key pairs on pile and sleeve compression struts evolve and brace against the confining tension ring of the sleeve (cf. [9]). Due to the local load introduction in front of the shear keys the grout is locally damaged (cf. [10]). The surrounding grout keeps the unbound material in place and so the load transfer maintains. Two main failure modes for the connection can be determined. Firstly, failure of the interface between steel and grout and secondly, failure of the grout.

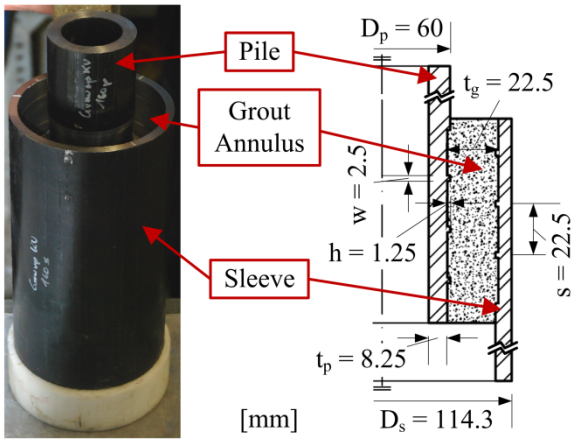

Figure 2: Geometry of the small scale grouted joint specimen

Within ‘GROWup’ a small scale specimen (cf. Figure 2), already employed in prior projects (cf. [11]), is used. Main aspect in the development of the specimen’s geometry was to investigate the filling material under multiaxial stress [12, 13]. To avoid buckling and global exceedance of the yield point in the steel tubes, they were chosen with a low slenderness. For a simple and reproducible manufacturing, the shear keys are turned out of the tube’s surface. As a result, they have a rectangular geometry and apply loads directly to the grout. In contrast to that shear keys made of weld beads have a smoother geometry and need some wedging to interlock with the grout. Nevertheless, the multiaxial stress state in the grout as well as the load bearing behaviour of the small scale specimen are in some extent comparable to real scale structures. Moreover, the specimen’s low costs compared to large scale specimens makes it possible to gain a broad range of test results.

The results presented afterwards are achieved with one industrial grout material showing the following properties:

- f_c ~90 MPa (118.3 MPa)
- f_t ~6 MPa (8.4 MPa)
- E ~ 40,000 MPa

Where f_c is the uniaxial compressive strength, f_t the uniaxial tensile strength and E the elastic modulus. The listed data are mean values, ascertained with 75 mm sample cubes. Independent tests conducted at the Institute of Building Materials Science, Leibniz University Hannover, Germany, revealed strength properties (values given in brackets) topping the listed manufacturer’s data (in front of brackets).

The grout material was prepared according to the manufacturer's instructions. After filling, the specimens were covered with foil and after 24 h of curing they were stored in a water basin at room temperature. They stayed in the water basin individually until they were tested.

3 STATE OF STANDARDISATION

The approving authority for the EEZ is the BSH (cf. [14]) and the design of OWTs must comply with the BSH-Standard [15]. Regarding grouted joints, the BSH-Standard refers to ISO 19902 [16] or DNV-OS-J101 [17].

3.1 Ultimate Limit State (ULS)

The ISO 19902 standard from the year 2007 originates from the oil and gas industry and the design regulations for grouted joints are based on investigations with low strength cement slurry [18]. Two ultimate limit states for the grouted connection under static load are defined. Firstly, the capacity of the interface between grout and steel $f_{g,sliding}$, including the radial stiffness of the connection K, a scale factor C_p, the presence of shear keys h/s and the compressive strength of the grout f_{cu} (cf. Equation (1)).

$$f_{g,sliding} = C_p \cdot \left[2 + 140 \cdot \left(\frac{h}{s} \right)^{0.8} \right] \cdot K^{0.6} \cdot f_{cu}^{\ 0.3} \tag{1}$$

Secondly, the shear capacity of the grout matrix $f_{g,shear}$, including the presence of shear keys h/s and also, the compressive strength of the grout f_{cu} (cf. Equation (2)).

$$f_{g,shear} = \left[0.75 - 1.4 \cdot \left(\frac{h}{s} \right) \right] \cdot f_{cu}^{\ 0.5} \tag{2}$$

The DNV-OS-J101 standard from the year 2013 focuses on OWTs. It includes design regulations for prevailingly axial loaded grouted joints in general and for jackets reference is made to the N-004 [19] standard also from 2013. The N-004 standard is a further stage of the ISO 19902 regulations with a different nomenclature and slightly different coefficients for the interface shear capacity f_{bks} (cf. Equation (3)).

$$f_{bks} = \left(\frac{800}{D_p} + 140 \cdot \left(\frac{h}{s} \right)^{0.8} \right) \cdot C_s^{\ 0.6} \cdot f_{ck}^{\ 0.3} \tag{3}$$

Since the grout matrix capacity is decisive in connections with shear keys, the N-004 result coincides with the calculation result according to ISO 19902 as shown for the small scale specimen in Figure 3.

The DNV-OS-J101 regulations also distinguish between the interface shear strength τ_{ks} (cf. Equation (4)) and the grout matrix capacity τ_{kg} (cf. Equation (5)).

$$\tau_{ks} = \frac{\mu \cdot E}{F} \cdot \left[\frac{h}{21 \cdot s} \cdot f_{ck}^{\ 0.4} \cdot \sqrt{\frac{t_p}{R_p}} \right] \cdot \frac{s}{L_g} \cdot N \tag{4}$$

For the interface capacity, besides stiffness ratio F, slenderness t_p/R_p, and overlapping length L_g, the surface friction μ between steel and grout is considered as well as shear key geometry h/s and number of shear keys N. Values for μ are given in the standard.

$$\tau_{kg} = \kappa \cdot f_{ck}^{\ 0.7} \cdot \left(1 - e^{-2L_g / R_p} \right) \tag{5}$$

The equation for the grout capacity considers the length of the connection L_g and the pile's radius R_p but not the shear keys. The overall static capacity is the highest of all available design regulations for the small scale specimen (cf. Figure 3).

A new and not standardized design approach for the static capacity is presented by Schaumann et al. [20] in 2012. This set of equations is based on the compression strut model by Lamport [9] and is supplemented with a consideration of the lateral confinement stress. The connection's capacity F_{sum} (cf. Equation (6)) is the sum of the capacity of one compression strut F_K (cf. Equation (7)), the corresponding horizontal capacity F_N (cf. Equation (8)), multiplied by the number of shear keys N. F_{sum} is also adjusted to non-linear effects for an increasing number of shear keys N by x and y (cf. [20]).

$$F_{sum} = \left(F_K + F_N \right) \cdot N \cdot y \cdot \left(\frac{h}{s} \right)^x \tag{6}$$

The capacity of one compression strut F_K includes the confined compressive strength of the grout material f_{cc} and geometric parameters.

$$F_K = f_{cc} \cdot h \cdot \pi \cdot \left(D_p + h \right) \tag{7}$$

And the corresponding horizontal capacity F_N includes, besides geometric parameters, the surface friction μ and the angle of the compression strut α.

$$F_N = \frac{F_K \cdot \left(t_g - h \right)}{\left[t_g \cdot \left(\tan \alpha - \mu \right) \right]} \tag{8}$$

This approach gives a medium capacity for the small scale specimen compared to current standards (cf. Figure 3).

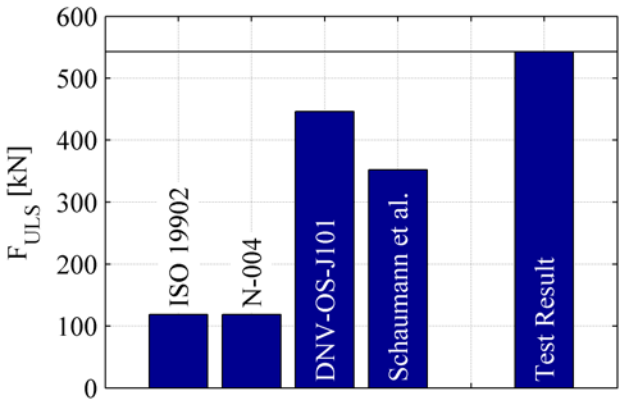

Figure 3: Grouted joint capacity of the small scale specimen according to different design regulations and test results

3.2 Fatigue Limit State (FLS)

In the ISO 19902 standard the fatigue limit is considered to be fulfilled if the maximum stress range does not exceed the sliding capacity of a grouted connection without shear keys (cf. Equation (9)). Thus, the existence of an endurance limit of the connection is assumed (cf. Figure 4).

$$f_{g,sliding} = C_p \cdot 2 \cdot K^{0.6} \cdot f_{cu}^{\ 0.3} \tag{9}$$

Since the regulations of the N-004 standard are based on the ISO 19902 standard, also an endurance limit of the connection is assumed to exist. But it is calculated as a reduction of the interface shear capacity f_{bks} by the factor 0.3 (cf. Equation (10)) and gives a higher fatigue limit for the small scale specimen compared to the ISO 19902 (cf. Figure 4).

$$P_{f,Rd} = \frac{0.3 \cdot f_{bks} \cdot D_p \cdot L_e}{\gamma_M} \tag{10}$$

For the fatigue limit state a linear damage accumulation is stated in DNV-OS-J101 (cf. Equation (11)).

$$\sum_{i=1}^{k} \frac{n_i}{N_i} \leq 1.0 \tag{11}$$

Hence, the DNV-OS-J101 regulations take into account the load cycle dependency (cf. Figure 4). The grout fatigue life is based on SN-curves (cf. Equation (12)) from pure material test data, considering the maximum and minimum occurring stress σ compared to the uniaxial grout strength f_{rd}.

$$\log_{10} N = C_1 \cdot \left(1 - \frac{\sigma_{max}}{f_{rd}}\right) \Big/ \left(1 - \frac{\sigma_{min}}{f_{rd}}\right) \tag{12}$$

Moreover, the SN-curves are available for different boundary conditions, likewise for submerged conditions, which is set by the parameter C_1. Thus, the DNV-OS-J101 can be assumed to provide the most progressive fatigue design procedure.

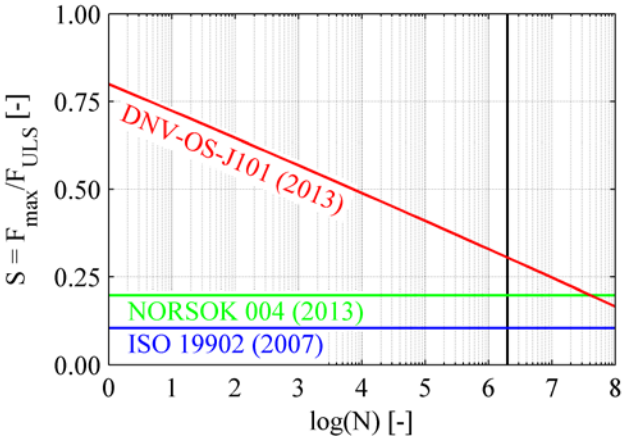

Figure 4: Characteristic SN-curves for the small scale specimen from different standards

3.3 Range of Application

Since all of the presented regulations were developed on the basis of different investigations with specific specimens and materials, they all have certain validity ranges. In Figure 5 a selection of these ranges is presented. Besides the geometric properties of the small scale specimen, two reference structures for typical jackets and tripods are classified. The reference structures were defined in cooperation with project partners and represent current designs. It shows that the reference jacket has typically low slenderness and therefore a high radial stiffness, whereas the reference tripod has higher slenderness and a lower radial stiffness. Both structures are close to the boundaries or outside the range of application. For the small scale specimen the slendernesses are even lower, due to the desired failure mode as described in section 2. The radial stiffness is comparable to the one of the reference jacket. But overall, the small scale specimen is outside of the range of application of current standards and so are current real structures. Consequently, the presented axial capacities are an estimate and the transferability of the small scale test results to real structures has to be investigated separately. Nevertheless, understanding the phenomena observed for the small scale specimen will help to understand the behaviour of real structures.

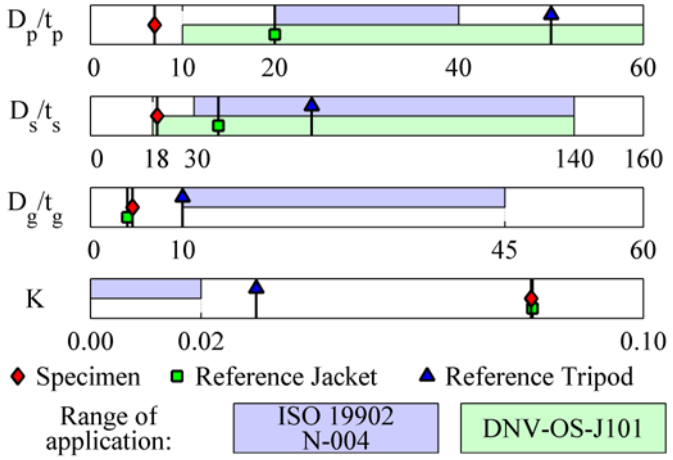

Figure 5: Range of application for different standards and classification of different grouted joint geometries

4 EXPERIMENTAL INVESTIGATIONS

4.1 Ultimate Limit State (ULS)

One batch of specimens consists of 16 similar specimens with the same filling material. When the grout reaches an age of 28 days, three small scale specimens per batch are investigated in a static loading test. The test is conducted displacement controlled with a velocity of 0.2 mm/min. On the one hand, these static tests show the quality of the specimens and manufacturing defects can be revealed. On the other hand, the maximum capacity F_{ULS} is determined as the mean value of the test results. This value is used as reference in the later fatigue investigations.

Moreover, the test results give significant insights in the load bearing behaviour of the structural detail. As presented in Figure 6 the load bearing behaviour can be divided into three different phases. Phase 1 describes the elastic deformation of the structural detail. An axial stiffness of the connection of C_{elas} ~ 640 kN/mm can be determined. At F ~ 300 kN (~ 55 % F_{ULS}) a small plateau (P1) evolves, first plastic deformations become visible and phase 2 begins. This result corresponds to the findings for other grout materials (cf. [21]). A second, wider plateau (P2) evolves at F ~ 400 kN (~ 73 % F_{ULS}). And finally, at F_{ULS} ~ 550 kN the maximum capacity is achieved (P3) and phase 3 begins. In phase 3 the displacements grow while the capacity reduces significantly.

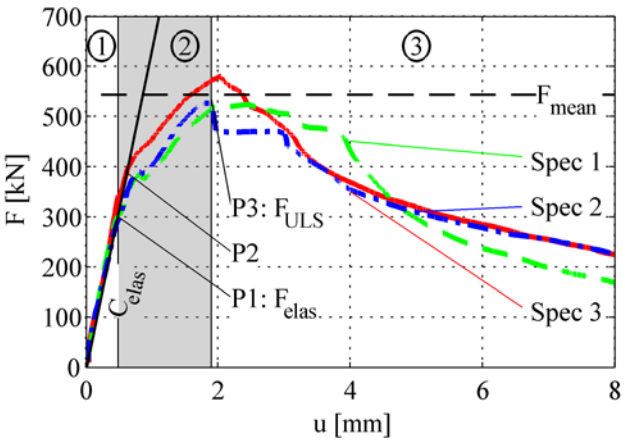

Figure 6: Force-displacement curves of the static axial capacity from three similar specimens

Figure 7 shows an opened specimen after a static loading test. Three cracks in the grout are clearly visible and can explain the described plateaus in the force-displacement curves.

The first crack evolves between shear key 4 (counted from top to bottom) on the pile surface and the lower, outer end of the grout. Since there is no opposite shear key on the inner sleeve surface this grout wedge cannot function as a compression strut, instead the loads applied by the inner shear key 4 are carried via tension to the shear key 4 on the sleeve surface. Due to the low tensile strength of the grout material this lower wedge will be detached at low load levels. After separation this wedge cannot transfer any load but sticks to the pile.

The second crack evolves between shear key 3 at the pile and shear key 4 at the sleeve. The resulting grout wedge can carry loads from the grout to the sleeve by surface friction. Exceeding stiction in this interface part will suddenly apply a higher load to the upper grout parts.

The third crack evolves between shear key 2 on the pile and shear key 3 on the sleeve. Within this wedge a compression strut between shear key 2 on the pile and shear key 4 on the sleeve can develop. As a result, the capacity of this wedge is limited by the compressive strength of the grout.

The resulting grout wedge on the upper end can also contain a compression strut between shear key 1 on the pile and shear key 3 on the sleeve. This part also fails due to the compressive strength of the grout.

After all cracks are developed and the compression struts failed the remaining capacity results from sliding friction and wedging of loose grout material.

It can be assumed that the cracks develop in the chronology of their number and that their growth corresponds to the plateaus in the force-displacement curve.

The presented results show that loads of 50 % F_{ULS} and below might cause no major cracks in the grout under static loads and might not reduce the elastic capacity of the structural detail.

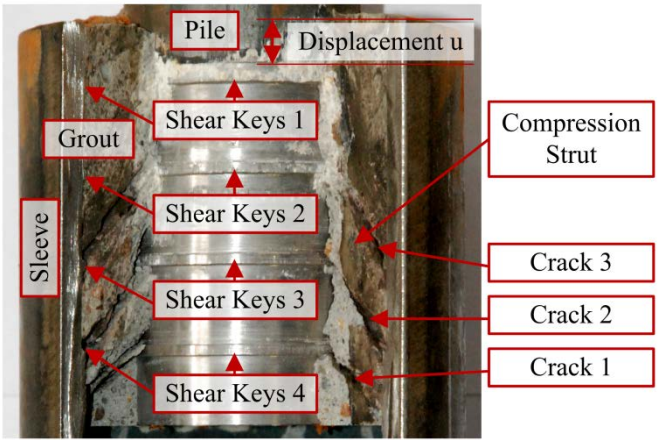

Figure 7: Open specimen after static loading test

4.2 Fatigue Limit State (FLS)

Test setup

The fatigue behaviour of the small scale grouted joints is investigated in the test rig presented in Figure 8. During the force controlled tests the applied load as well as the displacement of the load application plate is measured. For the displacement measurement three lasers in an arrangement of 120° around the plate are mounted. This measurement setup allows for recording only the axial displacement of the specimen and to subtract inclinations of the plate and displacements of the rig. To reduce the amount of data recorded, time frames of 5 seconds every 30 seconds are recorded with a rate of 100 Hz. As a result, the plots in logarithmic scales show different gaps at the beginning of the record (cf. Figure 9, 13 and 14).

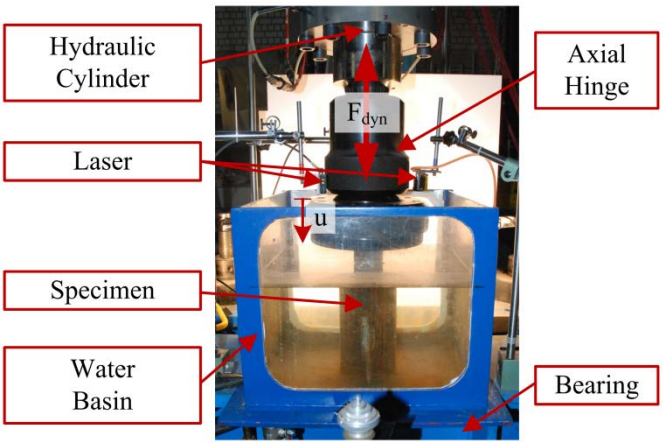

Figure 8: Fatigue test setup for submerged conditions

For tests in wet conditions the water basin is filled with tab water until the grout segment is fully submerged. A water overpressure like it acts on real structures in about 40 m water depth was not established. According to investigations by [5] the overpressure has only minor influence on the fatigue performance. All tests are conducted until the specimen's displacement exceeds the measuring range or the number of

applied load cycles reaches 2 million. The minimum compressive load is related to the maximum compressive load by R = 0.05.

The following three parameters were varied:

- Ambient condition (AC): dry / wet
- Maximum compressive load (F_{max}/F_{ULS}): 50 %, 25 %
- test frequency (f): 5.0 Hz, 1.0 Hz, 0.3 Hz

Twelve specimens were investigated in the fatigue tests.

Ambient conditions

Figure 9 shows the resulting displacement u plotted over the applied load cycles N for one specimen tested in dry and one tested in wet ambient conditions. The specimen in dry conditions reaches the cycle limit at 2 million load cycles with only slight stiffness degradation. In contrast to that, the specimen in wet conditions survives only 64,000 load cycles. Both specimens have in common that their stiffness degradation increases at about 1000 load cycles.

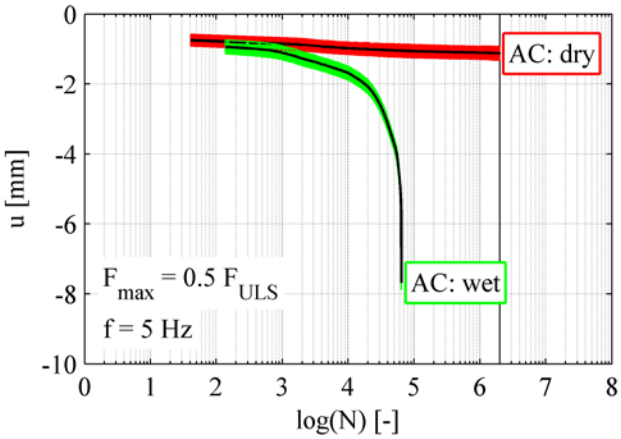

Figure 9: Load cycle dependent specimen displacement for two different ambient conditions

During the test in wet conditions, a significant amount of loose grout material deposited on top of the grout section as documented in Figure 10. In contrast to that only minor grout dust was found in the empty water basin after a specimen was tested in dry conditions.

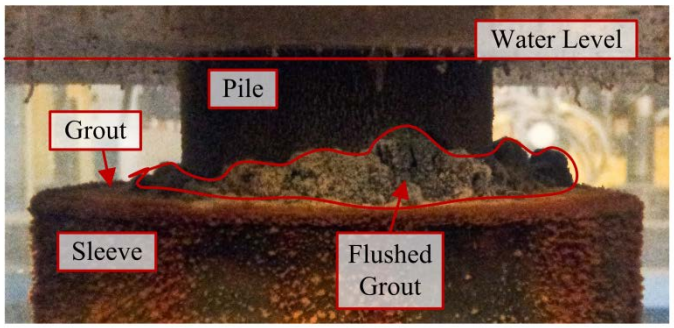

Figure 10: Flushed grout material on top of a specimen at the end of a submerged fatigue test

As described in section 2, local crushing of the grout in front of the shear keys is inevitable. Hence, loose grout material resides in the grout section. Elastic deformations of the steel tubes when loaded cause an opening of the contact interface in the boundary regions. In dry conditions no or only minor quantities of the loose grout material can get out of the grout section. This is the found grout dust. In wet conditions water can intrude into the interface openings. The alternating loading establishes a pumping process and water reaches the areas of loose material. As a result, the material is flushed out of the connection and deposits on top of the grout section. So, the volume of the grout in the connection reduces over time and the connection's stiffness decreases.

As mentioned before, both specimens tested in dry and wet ambient conditions show a stiffness decrease at about 1000 load cycles. Since the applied maximum compressive load is close to the end of the elastic range as described in section 2, it can be assumed that a crack due to fatigue, similar to the one when statically loaded, evolves in the grout at this point. Through this crack the water can intrude the grout significantly better and as a result the water leads to the pronounced stiffness degradation until the connection fails.

Local spalling of grout material due to pore water overpressure, as described by Nygard [8] for pure material tests, was not observed. But, since both specimens are stored in water until the tests were conducted, the moisture content in the surface region should be comparable and result in a similar impact.

For material fatigue tests conducted in dry ambient conditions, Holmen [22] and others depict a stiffness reduction of the secant modulus in the range of 10 % for high strength materials. The reduction is correlated to the number of applied load cycles. So this can be considered as a measure for the material degradation. As shown in Figure 11 this decrease cannot be observed for the structural fatigue tests, neither in dry nor in wet conditions. Reason for that can be the confining steel tube and thus, the multiaxial stress in the grout material. Hence, SN-curves from uniaxial grout material tests might not be directly applicable for multiaxial stress states. Though, it should be noted that the connection's elastic stiffness in the fatigue test is similar to the one in the static loading test (cf. Figure 6).

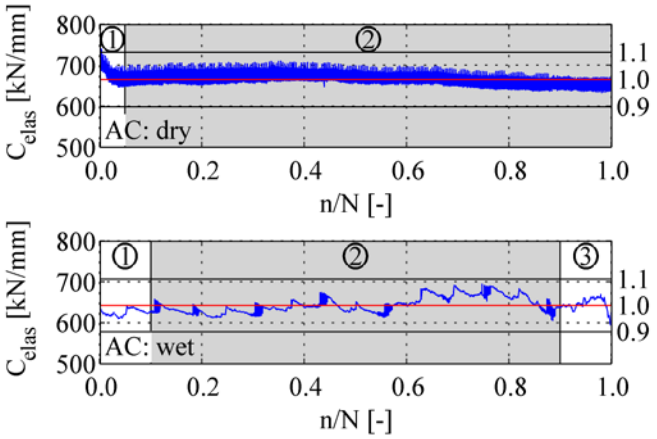

Figure 11: Elastic stiffness C_{elas} for two specimens in dry and wet ambient conditions

Figure 12 shows the static stiffness C_{stat} as the quotient of current mean force and mean displacement. The visible degradation process can be divided into three phases similar to the description for the static capacity in section 4. For the run out specimen tested in dry conditions, after a slight stiffness degradation in phase 1 until 5 % of the test period no further significant reduction is visible. Phase 3 is missing. In contrast to that, the specimen tested in wet conditions shows a greater stiffness decrease in phase 1 until 10 % of the test period. In phase 2 the stiffness decrease stabilizes but still continues until about 90 % of the test period. In phase 3 the specimen fails.

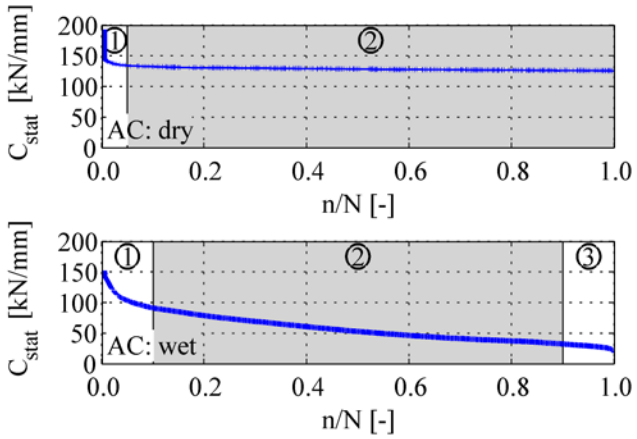

Figure 12: Static stiffness C_{stat} for two specimens in dry and wet ambient conditions

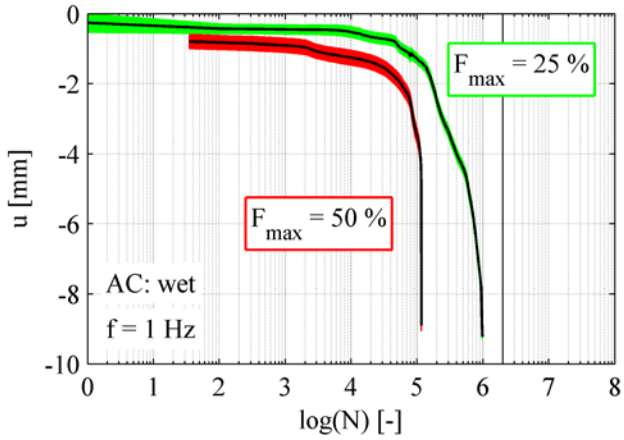

Figure 13: Load cycle dependent specimen displacement for two different maximum compressive loads

Maximum compressive load

Changing the maximum compressive load in wet conditions has a similar effect as in dry conditions. The results presented in Figure 13 show that a reduction of the maximum compressive load increases the number of endurable load cycles from 100,000 to about 1,000,000. It should be noted that the reduction of the maximum compressive load at a constant test frequency causes a reduction of the displacement velocity. Hence, besides the reduced utilization, the water pumping effects described before are slowed down and so is the material transport.

Test frequency

The first eigenfrequency of a jacket substructure is about 0.3 Hz [23]. Thus, the fatigue loads acting on grouted joints in real OWT structures mainly have this frequency. To realize an appropriate testing time frame, first tests were conducted at 5 Hz. In further tests the frequency was reduced to investigate its influence. The results in Figure 14 show an increase in the number of endurable load cycles from 64k at 5.0 Hz, over 100k at 1.0 Hz, to 160k at 0.3 Hz. Similar to the maximum compressive load, a lower frequency reduces the displacement velocity. For pure material tests contrary observations were made (cf. [6]). The loading frequency reduces attrition due to water, but not to a save level for the small scale specimen.

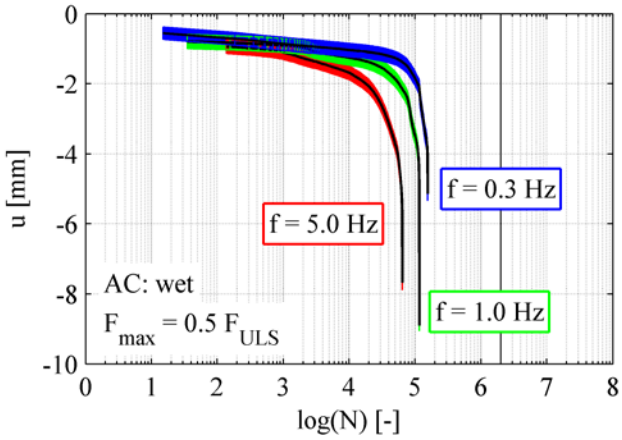

Figure 14: Load cycle dependent specimen displacement for three different test frequencies

5 CONCLUSIONS

The presented results show a significant influence of water to the fatigue performance of small scale grouted joint specimens. When loaded in submerged conditions, the specimens fail at much lower numbers of load cycles. This can be explained by water getting into the connection and flushing out loose grout material. The local stress peaks at the shear keys lead to local grout crushing and therefore, to moveable material particles. The material transport reduces the volume of the grout inside the connection and hence, the connection's stiffness. The transport process is correlated with the velocity of the load application. Maximum compressive load and test frequency influence the velocity of displacement and as a result the number of endurable cycles until failure.

Current design regulations are not directly applicable for the small scale specimen due to its geometric dimensions. Nevertheless, only the design regulations given in the DNV-OS-J101 standard provide a consideration of water effects for the fatigue design. These regulations are based on pure material tests. Results for the structural detail grouted joint show significantly different behaviour compared to pure uniaxial material tests. Reason for that might be the structural influence and the resulting multiaxial stress state in the grout.

Since the small scale specimens are not exactly to scale to real structures the transferability of the presented results to real dimensions is questionable and will be part of further research.

ACKNOWLEDGMENTS

The presented results are achieved within the research project ‘GROWup – Grouted Joints for Offshore Wind Energy Converters under reversed axial loadings and up scaled thicknesses’ (funding sign: 0325290) funded by the German Federal Ministry for the Environment, Nature Conservation and Nuclear Safety (BMU). The research partners are Institute for Steel Construction and Institute of Building Materials Science, both at Leibniz University Hannover, Germany. The authors thank the BMU for the funding and all accompanying industry project partners (Fraunhofer IWES, GL Germanischer Lloyd, Senvion, RWE Innogy, STRABAG) for their support.

REFERENCES

[1] Schaumann, P.; Raba, A. and Bechtel, A.: “Impact of Contact Interface Conditions on the Axial Load Bearing Capacity of Grouted Connections”, in *Proceedings of EWEA 2013*, Vienna, Austria, 2013.

[2] Allnoch, N.: Overview of German Offshore Wind Farms (in German). Internationales Wirtschaftsforum Regenerative Energien. Available: www.offshore-windenergie.net/windparks (2013, Dec. 28).

[3] Deutschlands Zukunft gestalten: Koalitionsvertrag zwischen CDU, CSU und SPD - 18. Legislaturperiode (in German). Available: http://www.tagesschau.de/inland/koalitionsvertrag152.pdf (2013, Dec. 16).

[4] German Maritime and Hydrographic Agency: “Spatial Offshore Grid Plan for the German Exclusive Economic Zone of the North Sea and Non-technical Summary of the Environmental Report 2012”, Comprehensive Summary, Hamburg, Germany, 2013.

[5] Waagaard, K.: “Fatigue of Offshore Concrete Structures: Design and Experimental Investigations”, in *9th Annual Offshore Technology Conference*, Houston, Texas, USA, pp. 341–350, 1977.

[6] Waagaard, K.: “Experimental Investigation on the Fatigue Strength of Offshore Concrete Structures”, in *9th Annual Energy Technology Conference*, New Orleans, USA, pp. S. 73-81, 1986.

[7] Nishiyama, M.; Muguruma, H. and Watanabe, F.: “On the Low-cycle Fatigue Behaviours of Concrete and Concrete Members under Submerged Condition”, 1987.

[8] Nygaard, K.; Petkovic, G. and Rosseland, S, et al.: “High Strength Concrete, SP3 - Fatigue: Report 3.1: The Influence of Moisture Conditions on the Fatigue Strength of Concrete”, SINTEF Structural Engineering - FCB, Trondheim, Norway, 1992.

[9] Lamport, W. B.: “Ultimate Strength of Grouted Pile-to-Sleeve-Connections”, Dissertation, University of Texas at Austin, Austin, Texas, USA, 1988.

[10] Krahl, N. W. and Karsan, D. I.: “Axial Strength of Grouted Pile-to-Sleeve Connections”, *Journal of Structural Engineering*, Vol. 111, No. 4, pp. 889–905, 1985.

[11] Schaumann, P. and Wilke, F.: “Fatigue Assessment of Support Structures of Offshore Wind Energy Conversion Systems”, in *Annual Report 2005*, P. Schaumann and J. Peinke, Eds, Hannover, Germany, pp. 36–39, 2006.

[12] Wilke, F.: “Load Bearing Behaviour of Grouted Joints Subjected to Predominant Bending”, Dissertation, Institute for Steel Construction. Leibniz University Hannover, Hannover, Germany, 2014.

[13] Lochte-Holtgreven, S.: “Zum Trag- und Ermüdungsverhalten beigebeanspruchter Grouted Joints in Offshore-Windenergieanlagen (On Load Bearing and Fatigue Behaviour of Grouted Joints in Offshore Wind Turbines Subjected to Bending)”, Dissertation, Institute for Steel Construction. Leibniz University Hannover, Hannover, Germany, 2013.

[14] Lohaus, L.; Schaumann, P. and Lochte-Holtgreven, S, et al.: “Zustimmungen im Einzelfall für Grout-Verbindungen in Tragstrukturen für die Offshore-Windenergie (Approval in the Individual Case for Grouted Connections in Substructures for the Offshore Wind Energy)”, *Bautechnik*, Vol. 90, No. 7, pp. 402–409, 2013.

[15] BSH D-OWT: Standard - Design of Offshore Wind Turbines. German Maritime and Hydrographic Agency, June 2007.

[16] DIN EN ISO 19902: Petroleum and Natural Gas Industries - Fixed Steel Offshore Structures (in German). DIN Deutsches Institut für Normung e.V, July 2008.

[17] DNV-OS-J101: Design of Offshore Wind Turbine Structures. Det Norske Veritas, January 2013.

[18] Harwood, R. G.; Billington, C. J. and Buitrago, J, et al.: “Grouted Pile to Sleeves Connections: Design Provisions for the New ISO Standard for Offshore Structures”, in *Proceedings of the 15th Ocean, Offshore & Arctic Engineering Conference*, Florence, Italy, pp. 1–12, 1996.

[19] N-004: Design of Steel Structures. Norsok Standard, February 2013.

[20] Schaumann, P.; Bechtel, A. and Lochte-Holtgreven, S.: “Nachweisverfahren zur Tragfähigkeit überwiegend axial beanspruchter Grouted Joints in Offshore-Tragstrukturen (Design Procedure for the Capacity of Prevailingly Axially Loaded Grouted Joints in Offshore Substructures)”, *Stahlbau*, Vol. 81, No. 9, pp. 679–688, 2012.

[21] Schaumann, P.; Bechtel, A. and Lochte-Holtgreven, S.: “Fatigue Design for Prevailing Axially Loaded Grouted Connections of Offshore Wind Turbine Support Structures in Deeper Waters”, in *Proceedings of EWEC 2010*, Warsaw, Poland, 2010.

[22] Holmen, J. O.: “Fatigue of concrete by constant and variable amplitude loading”, Dissertation, Norwegian Institute of Technology. University of Trondheim, Trondheim, Norway, 1979.

[23] Schaumann, P.; Böker, C. and Wilke, F.: “Lebensdaueranalyse komplexer Tragstrukturen unter Seegangsbeanspruchung (Life Cycle Analysis for Complex Substructures in Maritime Loading)”, *Stahlbau*, Vol. 74, No. 6, pp. 406–411, 2005.

